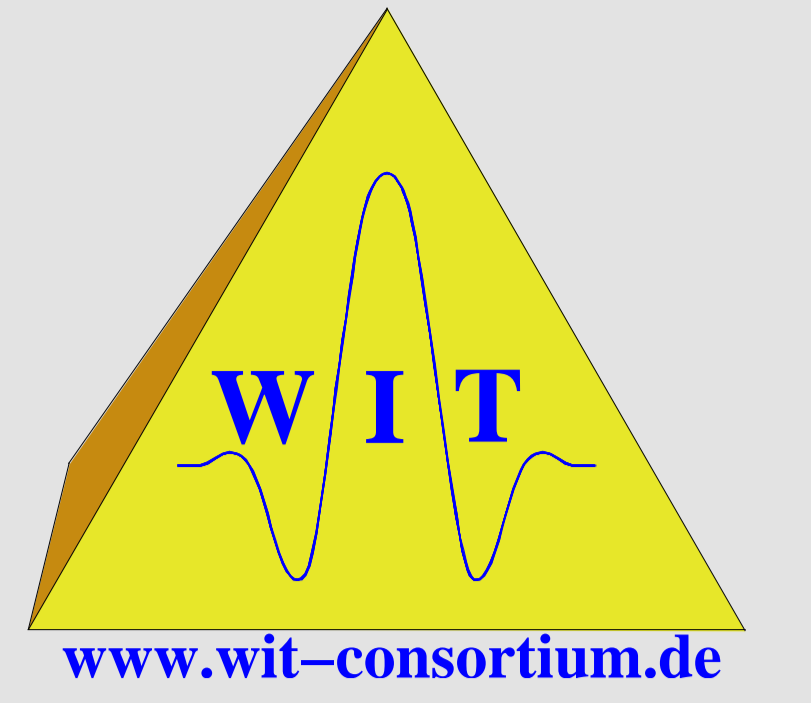


CRS-stack-based seismic reflection imaging – a real data example

Z. Heilmann, J. Mann, E. Duveneck and T. Hertweck
Geophysical Institute, University of Karlsruhe, Germany



Summary

In recent years, it was often demonstrated that the *Common-Reflection-Surface* (CRS) stack produces reliable stack sections with high resolution and excellent signal-to-noise ratio. Moreover, an entire set of physically interpretable stacking parameters, so-called kinematic wavefield attributes, is determined as a by-product of this data-driven imaging process. These CRS attributes may be even more important than the stack section itself because they can be applied in further processing to solve a number of dynamic and kinematic stacking, modeling, and inversion problems. Utilizing them, a sophisticated and highly flexible seismic reflection imaging workflow can be established leading from the preprocessed multicoverage data in the time domain to migrated sections in the depth domain (Mann et al., 2003; Hertweck et al., 2003). For this case study, a CRS-stack-based imaging workflow was applied in a recent exploration project—leading to superior results compared to a standard processing sequence consisting of normal- and dip-moveout corrections (NMO/DMO) and stack with subsequent time migration and depth conversion.

Introduction

Obtaining a sufficiently accurate image, either in time or in depth domain, is often a difficult task, especially in regions with complex geological structure or for data with low signal-to-noise (S/N) ratio. Therefore, it is advisable to extract as much information as possible directly from the measured data. The ongoing increase in available computing power makes so-called data-driven approaches (e. g., Hubral, 1999) feasible, which, thus, have increasingly gained in relevance. The Common-Reflection-Surface (CRS) stack (e. g., Müller, 1999; Jäger et al., 2001; Mann, 2002) is one of these methods. Besides an improved zero-offset (ZO) simulation, its decisive advantage is that an entire set of kinematic wavefield (or CRS) attributes is obtained. These attributes can be used

- for the determination of a macrovelocity model via CRS-attribute-based tomographic inversion (Duveneck, 2004).
- to estimate physical properties of the wavefield like, e. g., the geometrical spreading factor (Vieth, 2001) or the projected Fresnel zone (Mann, 2002).
- to distinguish between reflection and diffraction events (Mann, 2002).
- to determine optimal apertures for stacking and migration.
- to perform an automatic time migration (Mann, 2002).
- to handle top-surface topography (Heilmann, 2003).
- for residual static corrections using CRS operators (Koglin and Ewig, 2003).

The seismic data used for this case study was acquired in 2003 in the close vicinity of Karlsruhe, Germany:

Shot & receiver geometry		Midpoint & offset geometry	
Number of shots	213	Number of CMP bins	413
Shot interval	50 m	Maximum CMP fold	199
Number of receivers	240	CMP bin interval	25 m
Receiver interval	50 m	Maximum offset	±10 km
Recording parameters		Frequency content	
Recording time	5 s	Dominant frequency	35 Hz
Sampling interval	2 ms	Maximum frequency	100 Hz

The acquisition was performed with the intention to obtain a structural image of the subsurface relevant for a projected geothermal power plant. The latter will be based on two boreholes reaching a depth of ≈ 2.5 km, where a strongly fractured horizon of hot-water-saturated limestone is located. As the achievable production rate depends mainly on the number of faults reached by the partly deflected boreholes, a detailed knowledge of the local subsurface structure is essential.

Standard processing sequence applied by a contractor:

- NMO/DMO/stack
- finite-differences (FD) time migration
- time-to-depth conversion using a macrovelocity model based on stacking velocities.

In parallel to this, we applied the CRS-stack-based imaging sequence depicted in Figure 1. The individual steps and their results are discussed in the following sections.

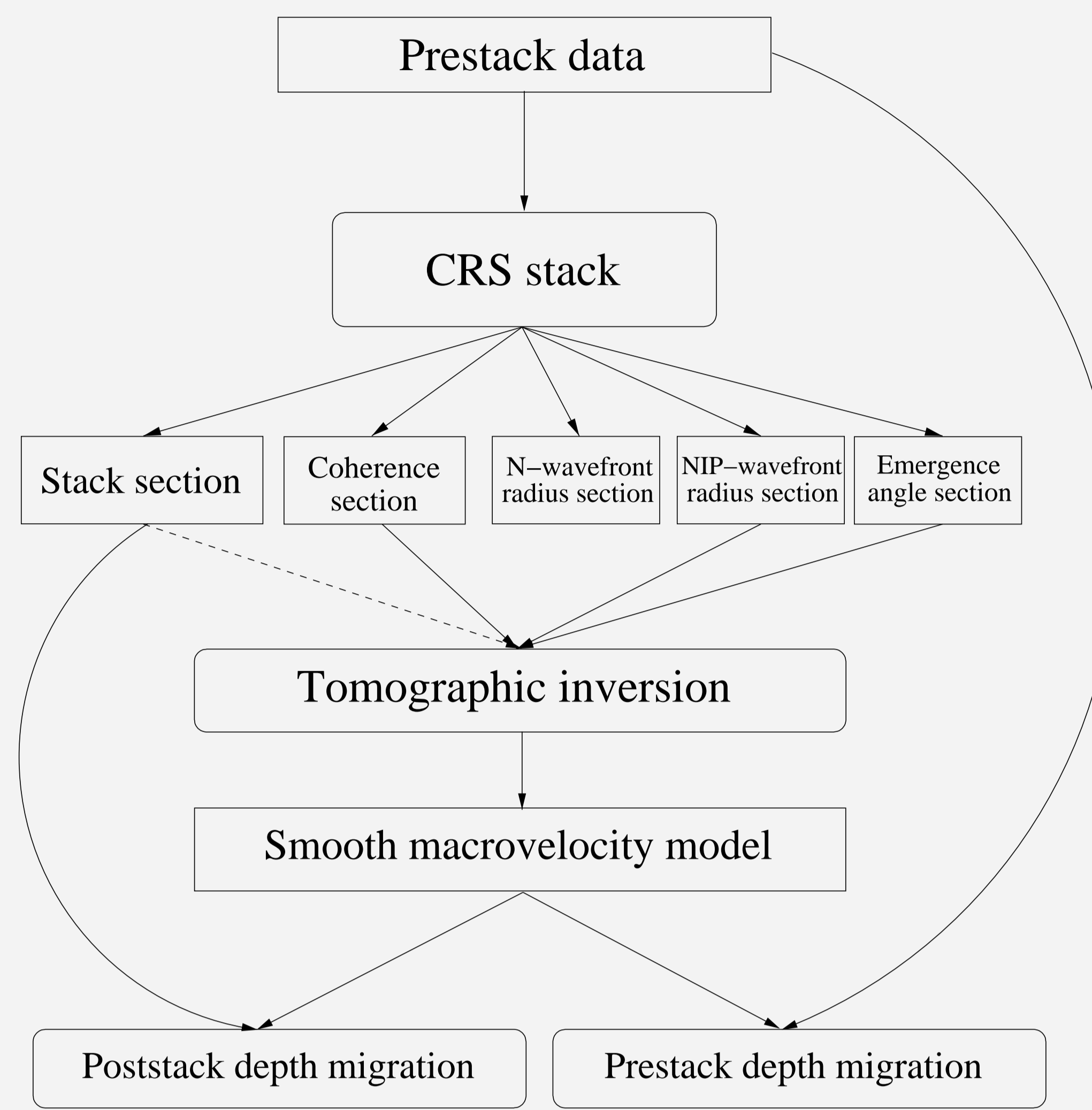


Figure 1: CRS-stack-based imaging workflow

CRS stack

Basic features of the CRS stack for 2-D ZO simulation:

- a *spatial* stacking aperture is used \Rightarrow higher stability and signal-to-noise ratio compared to conventional methods.
- a generalized coherence-based velocity analysis is performed *automatically* at *every* ZO location \Rightarrow the ZO section is produced in a purely *data-driven* way.
- provides three kinematic wavefield attributes for every ZO sample \Rightarrow information valuable for further processing extracted as by-product.

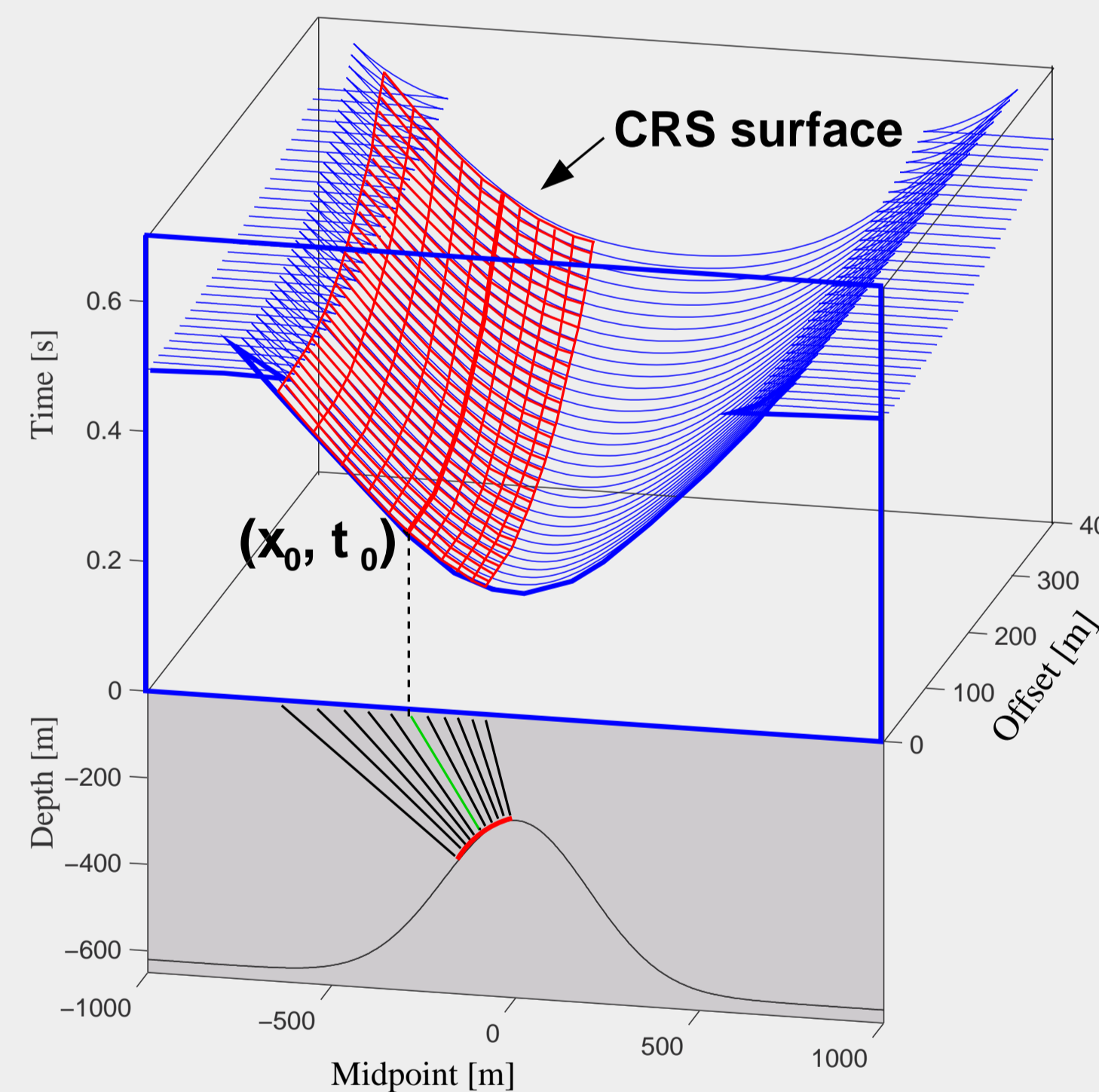


Figure 2: Comparison between the CRS stacking operator (red) that corresponds to the central ray (green) and its paraxial vicinity and the real traveltimes response of the reflector (blue).

Expressed in terms of midpoint coordinate x_m and half-offset h , the second-order traveltimes approximation used as CRS stacking operator (Figure 2) reads

$$t_{\text{hyp}}^2(x_m, h) = \left[t_0 + \frac{2 \sin \alpha (x_m - x_0)}{v_0} \right]^2 + \frac{2 t_0 \cos^2 \alpha}{v_0} \left[\frac{(x_m - x_0)^2}{R_N} + \frac{h^2}{R_{\text{NIP}}} \right],$$

where v_0 represents the near-surface velocity and (t_0, x_0) is the considered ZO location. This operator is parameterized by three kinematic wavefield attributes defined at the surface location x_0 , which are,

- α , the emergence angle of the central ray,
- R_{NIP} , the radius of the normal-incidence-point (NIP) wavefront, and
- R_N , the radius of the normal wavefront.

These attributes are related to the local properties of a reflector segment in depth, namely its location, dip, and curvature, by means of two hypothetical eigenwave experiments (see, e. g., Jäger et al., 2001).

Within the course of this project, the CRS stack method was complemented by an algorithm smoothing the obtained CRS attributes in an event-consistent way. Afterwards, the smoothed attributes were used for a final optimization and stacking iteration, resulting in a significant enhancement of event continuity. The final stack was restricted to the projected first Fresnel zone calculated from the obtained CRS attributes.

The simulated ZO section, the coherence section, and two (of three) attribute sections are shown in Figures 2-5. The coherence indicates the fit between the determined CRS stacking operators and the reflection events in the prestack data. Attribute values associated with very low coherence values are masked out (black), as they are not expected to be reliable.

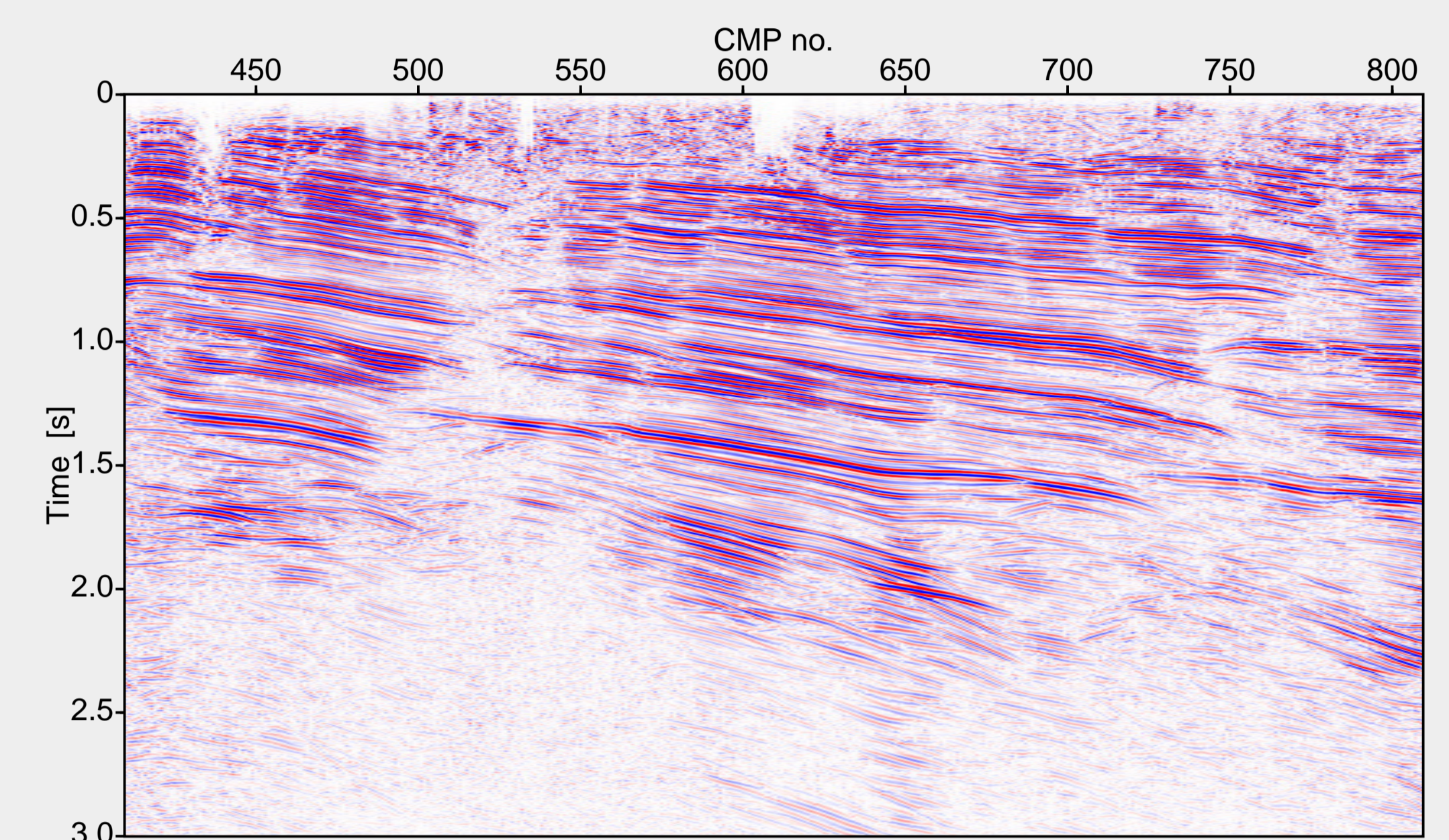


Figure 3: Simulated zero-offset section.

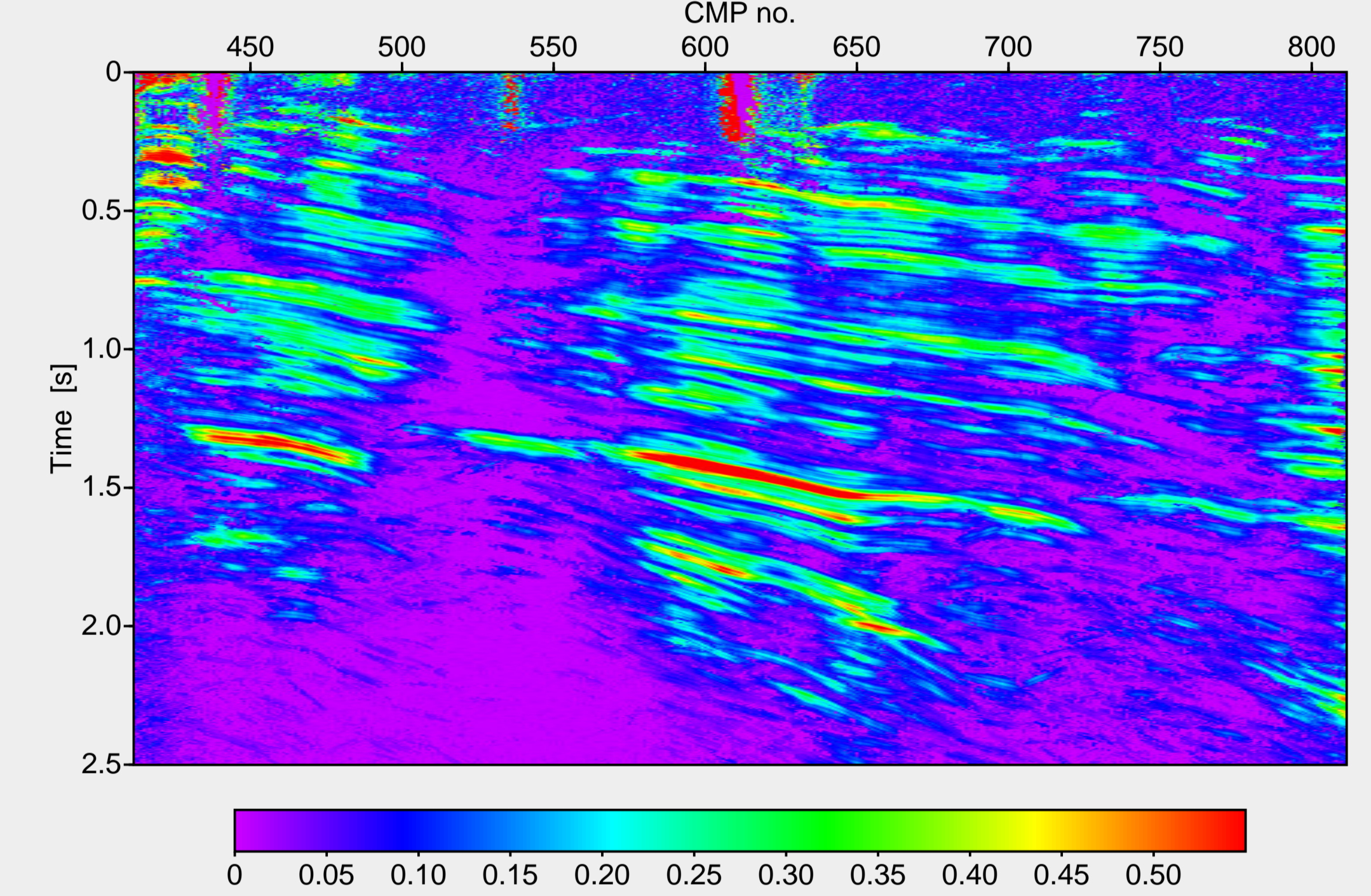


Figure 4: Coherence section.

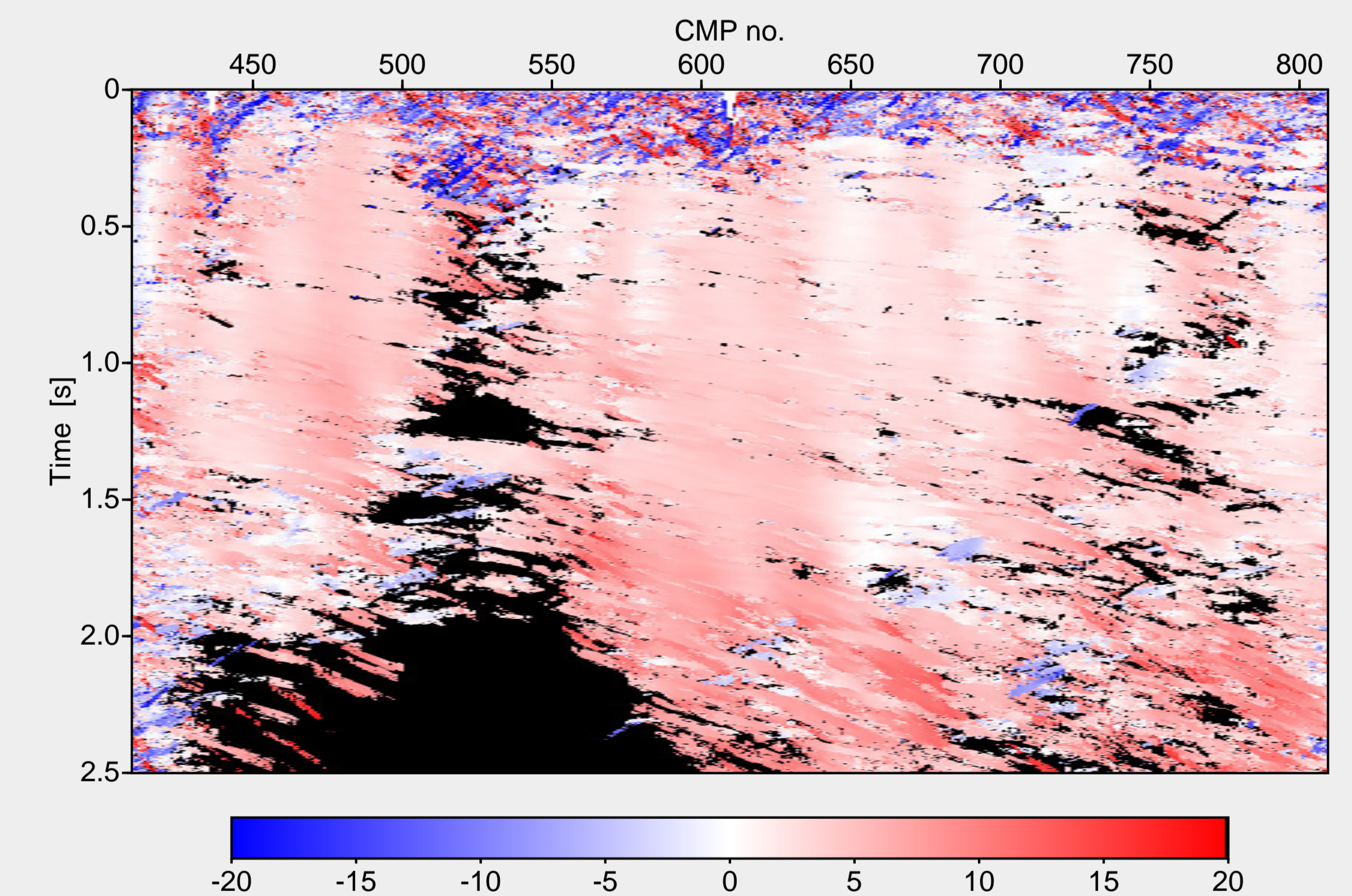


Figure 5: Emergence angle section, α [°].

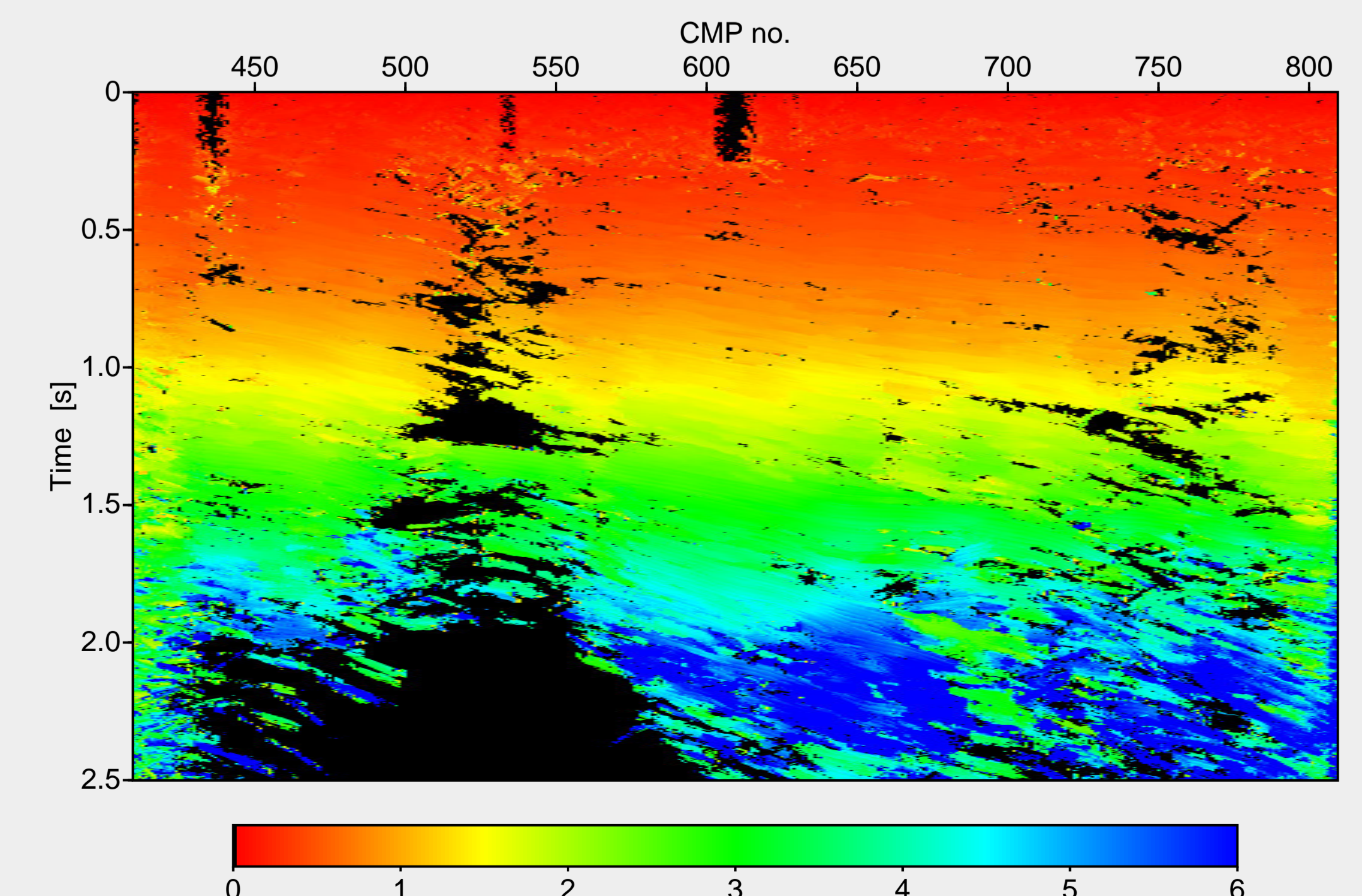
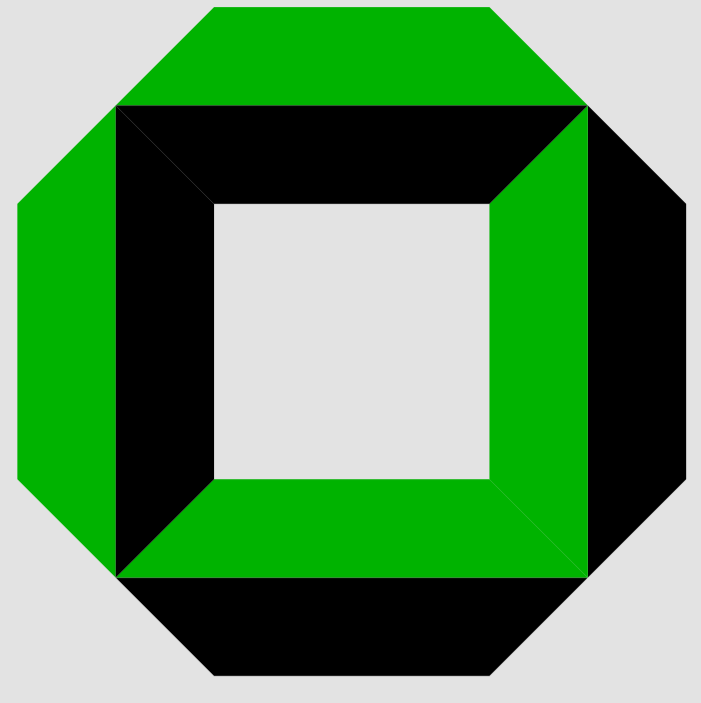
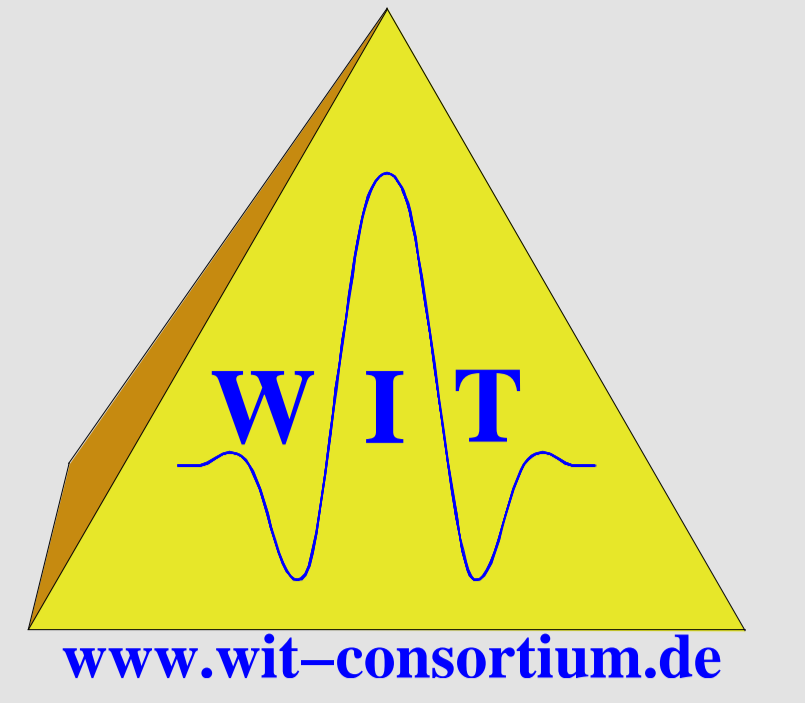


Figure 6: NIP-wavefront radius section, R_{NIP} [km].



CRS-stack-based seismic reflection imaging – a real data example

Z. Heilmann, J. Mann, E. Duvencek and T. Hertweck
Geophysical Institute, University of Karlsruhe, Germany



Tomographic inversion

Bridging the gap between time and depth domain is one of the crucial steps in seismic data processing. A macrovelocity model needs to be estimated, in order to achieve a depth image from the time domain pre- and/or poststack data. Fortunately, such a model can be obtained directly from the CRS stack results: the attributes R_{NIP} and α related to the NIP wave at a given ZO location describe the approximate multi-offset reflection response of a common-reflection point (CRP) in the subsurface. Therefore, the NIP wave focuses at zero traveltimes at the NIP, if propagated into the subsurface in a correct model. This principle can be utilized for an inversion that uses the above-mentioned attributes picked in the CRS-stacked section to obtain a laterally inhomogeneous velocity model. The CRS-stack-based velocity determination approach is realized as a tomographic inversion (Duvencek and Hubral, 2002; Duvencek, 2004), in which the misfit between picked and forward-modeled attributes is iteratively minimized in the least-squares sense. The velocity model is defined by B-splines, i. e., a smooth model without discontinuities is used which is well suited for ray-tracing applications.

In this case study, about 1000 ZO samples together with their respective attribute values were picked in order to achieve an appropriate resolution and reliability. To reduce the effort involved in manual picking, the existing software was extended by a module performing automatic picking based on the coherence associated with the ZO samples. The picked data were checked, using several criteria in order to discriminate outliers and attributes related to multiples, before the tomographic inversion process was applied. The determined velocity model is displayed in Figure 7.

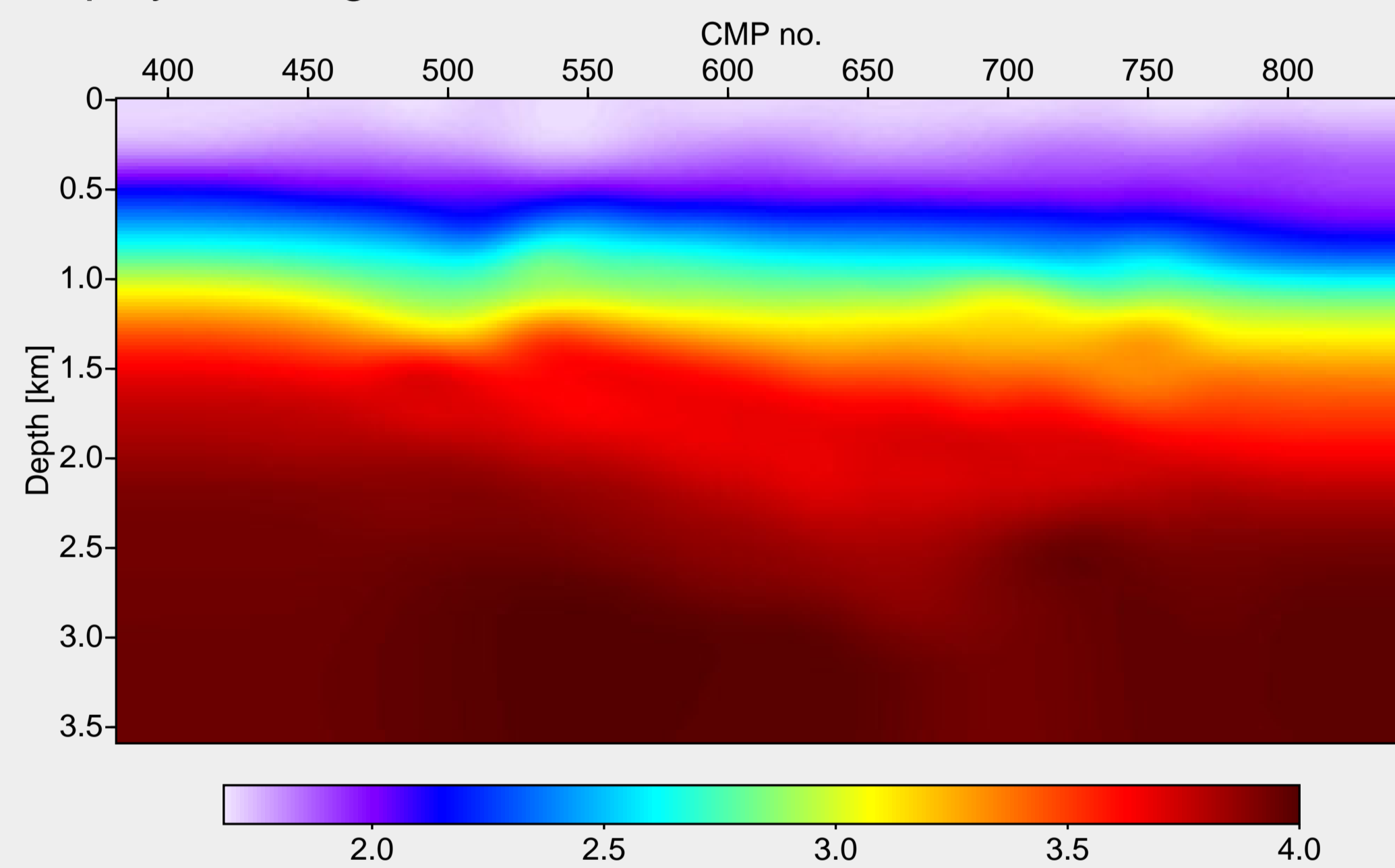


Figure 7: Macrovelocity model [km/s]

Depth migration

Based on the macrovelocity model obtained in the previous step, a Kirchhoff-type prestack depth migration (PreSDM) was carried out, in which offsets up to 3 km were considered. The necessary kinematic Green's function tables (GFTs) were calculated by means of an eikonal solver. The resulting depth-migrated prestack data were firstly muted to avoid excessive pulse stretch for shallow reflectors and then stacked in offset direction in order to obtain the subsurface image displayed in Figure 8.

Some common-image gathers (CIGs) are displayed in Figure 9, where the muting can be seen directly. As most of the events in the CIGs are flat, we can state that the estimated macrovelocity model is kinematically consistent with the data. Note that no velocity model refinement was applied after the PreSDM.

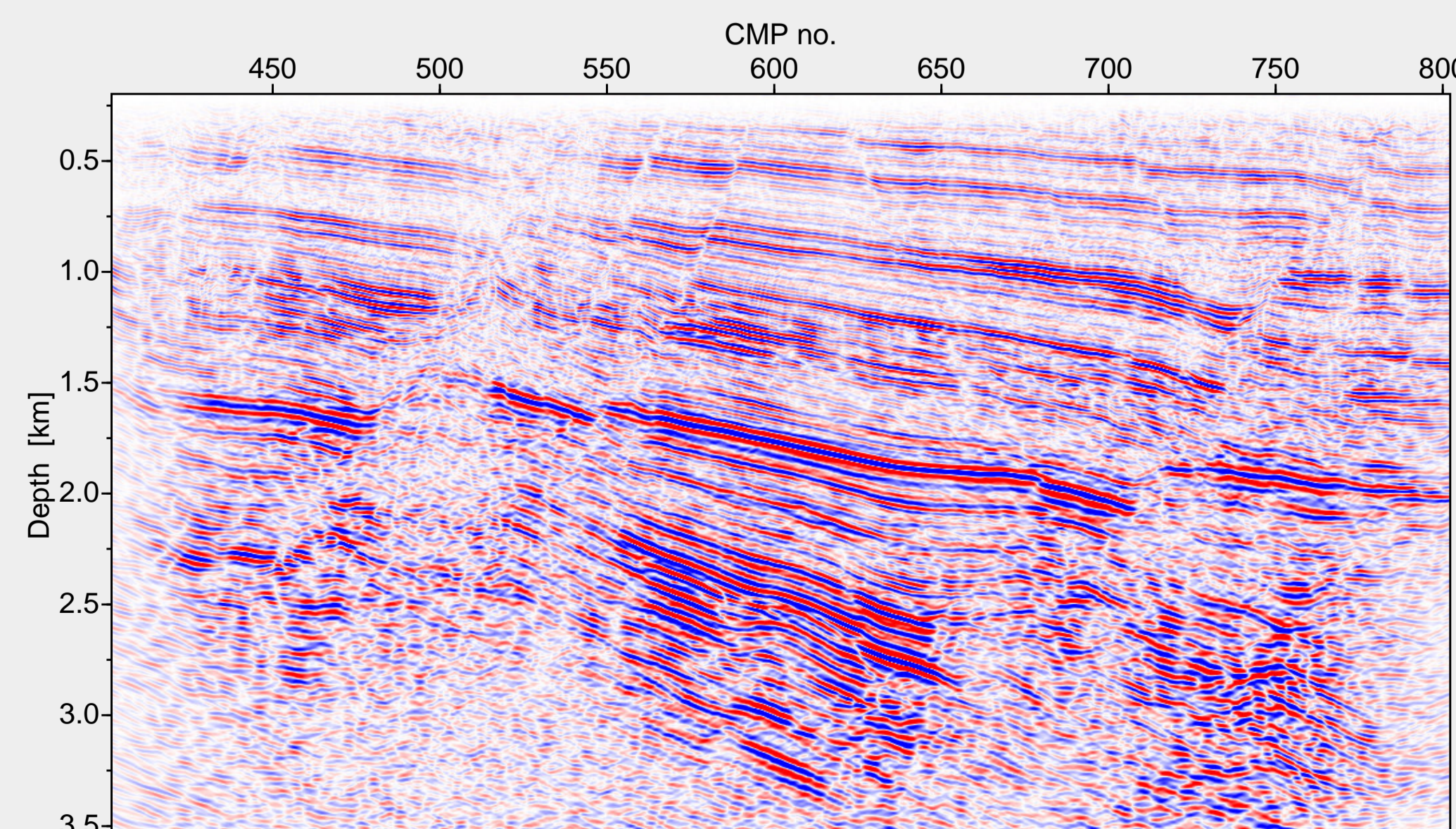


Figure 8: Prestack depth migration result

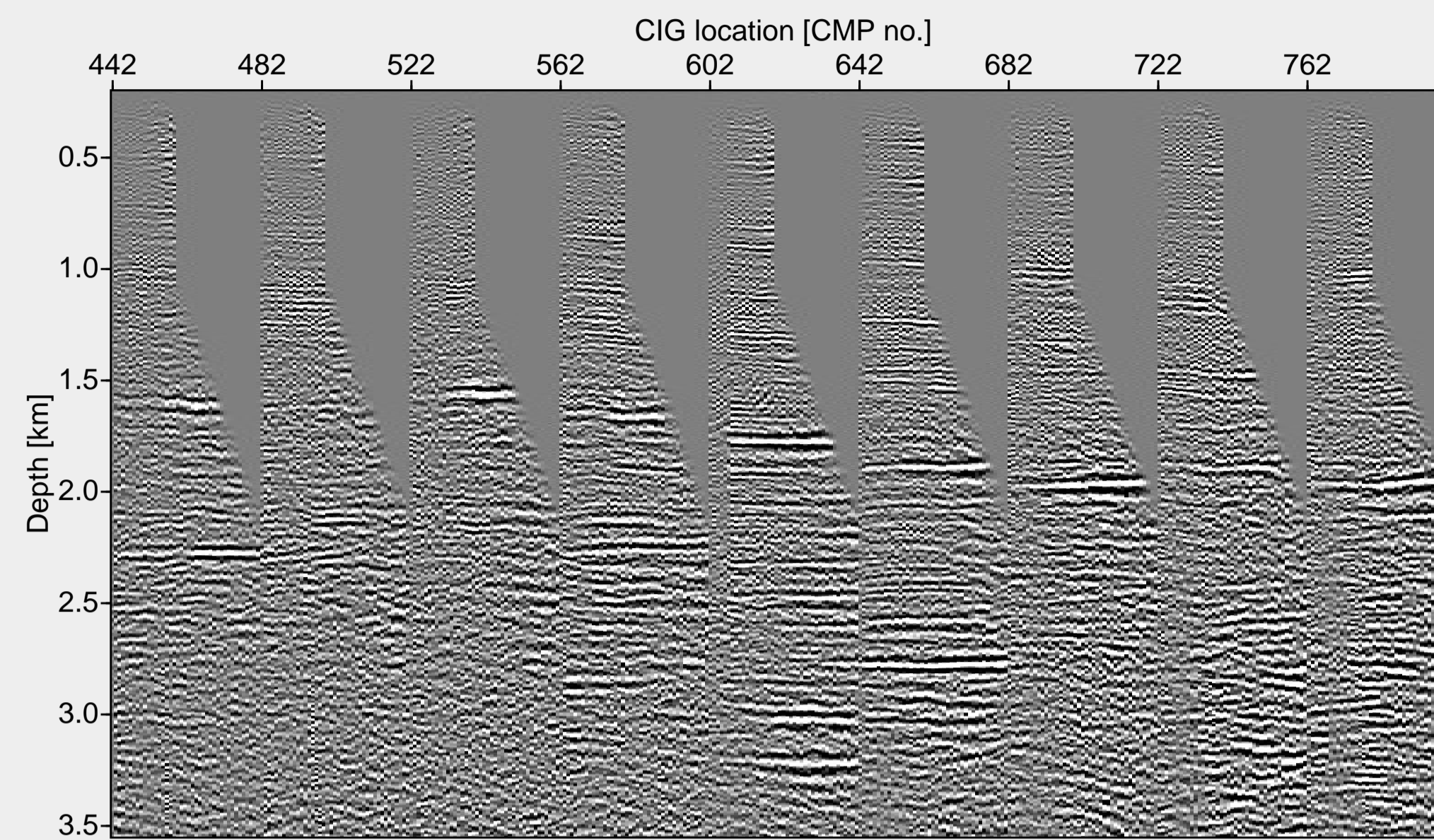


Figure 9: Common-image gathers

As a complementary or alternative step of our CRS-stack-based imaging workflow a Kirchhoff-type poststack depth migration (PostSDM) was performed using the CRS-stacked section and the determined macrovelocity model. The result is shown in Figure 10.

Due to the fact that, unlike as for prestack migration, only the stacked ZO section is migrated to depth, the computational costs of the PostSDM were about 60 times lower than those of the PreSDM. Generally, PostSDM can be advantageous in cases of moderate structural complexity and/or poor S/N ratio.

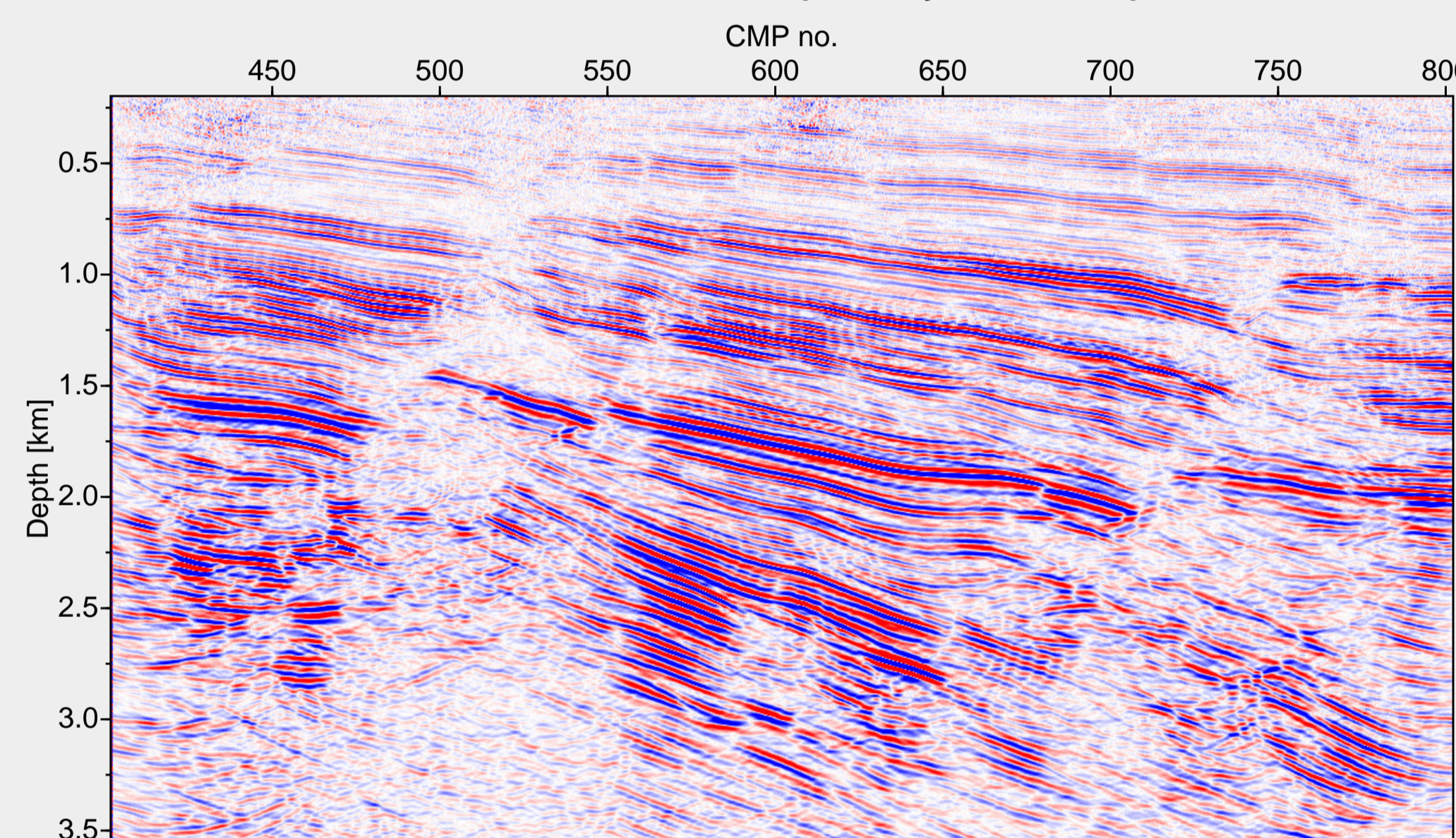


Figure 10: Poststack depth migration result

Discussion

The Post- as well as the PreSDM results show a good agreement to existing borehole data. Many structural details can be observed, e.g., :

- various faults and vertical offsets of reflectors.
- deflection and fracturing of reflectors.
- changes of reflector characteristics across faults.

Comparing the Pre- and PostSDM results reveals that in this case, in which the S/N ratio is high and the subsurface structure rather complex, PostSDM cannot fully compete with PreSDM in view of resolution and image quality. In particular:

- the faults are clearer resolved by the PreSDM and
- the shallow area (depth < 750 m) is better imaged.

Nevertheless, there are also regions, especially at greater depth, where some structures are better resolved by the PostSDM. ⇒ The PostSDM result provides helpful complementary information. Both migrated sections are used for the final geological interpretation.

A preliminary interpretation is shown in Figure 11. It was performed to determine structure and faulting and is only a small fraction of what may be accomplished by a quantitative interpretation of, e. g., reflector characteristics.

From the interpreter's point of view (HotRock EWK Offenburg/Pfalz GmbH), the CRS-stack-based imaging results have some major advantages compared to the standard processing results (not shown here):

- Generally higher resolution of reflectors and faults, particularly in the target area.
- Lateral variations in reflector characteristics can easier be observed.
- More reliable depth location of reflectors, according to well data and other geological and geophysical information.
- Faults may be traced from near-surface up to a depth of about 3 km.

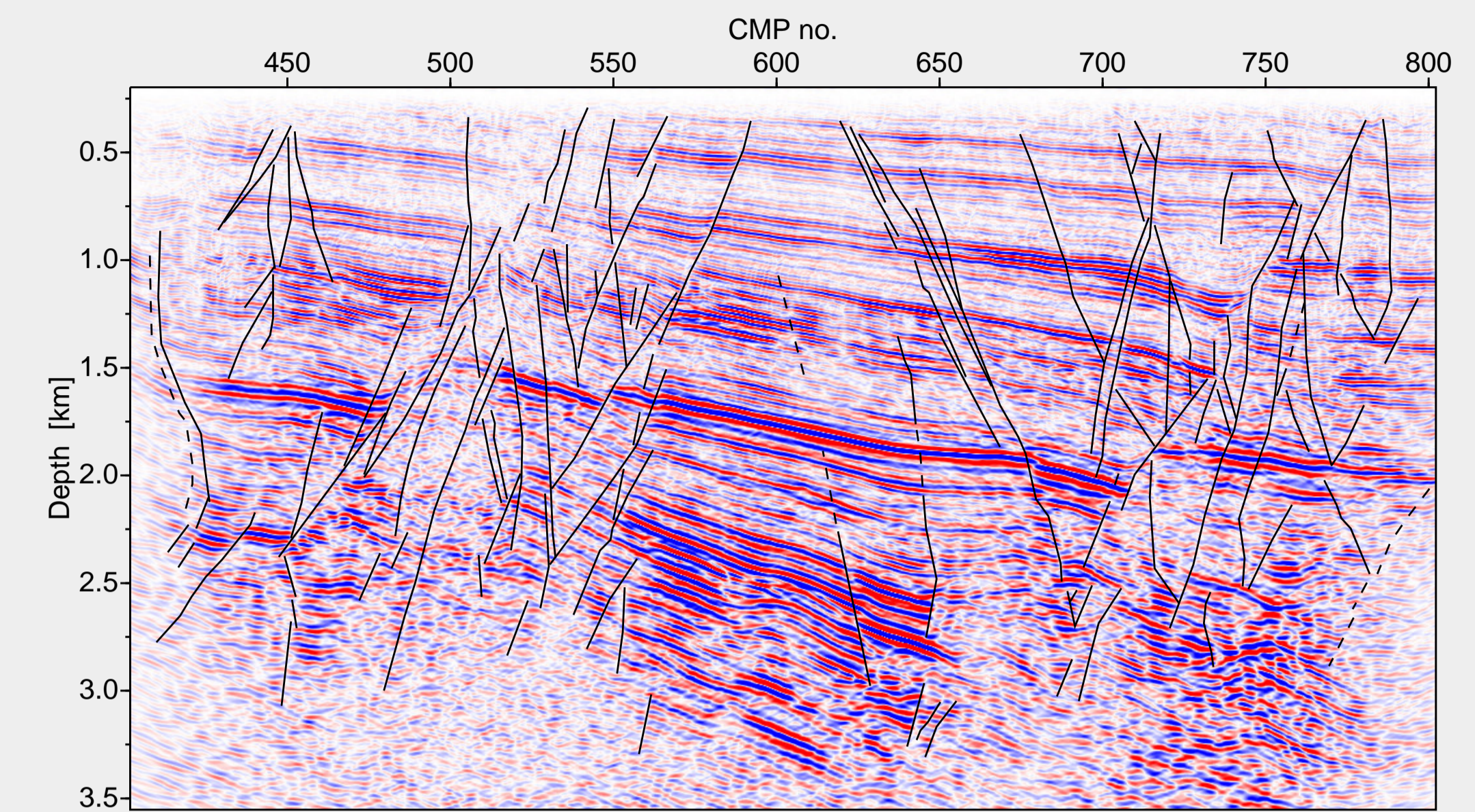


Figure 11: Preliminary structural interpretation

Conclusions

The great potential of our seismic imaging approach based on kinematic wavefield attributes obtained by the CRS stack was demonstrated in a recent exploration project.

Due to the fact that a standard processing sequence was carried out in parallel, the reliability and high quality of the results of our imaging workflow could be proven.

The target area and particularly the existing faults were imaged clearly. This verified the high grade of tectonic displacement necessary to ensure a sufficiently large production rate of the projected geothermal power plant.

⇒ With the obtained results, a good basis for the final geological interpretation and a successful drilling is available.

References

- Duvencek, E. (2004). Velocity model estimation with data-derived wavefront attributes. *Geophysics*, 69:265–274.
- Duvencek, E. and Hubral, P. (2002). Tomographic velocity model inversion using kinematic wavefield attributes. 72nd Ann. Internat. Mtg., Soc. Expl. Geophys., Expanded Abstracts. Session IT 2.3.
- Heilmann, Z. (2003). Extensions of the Common-Reflection-Surface Stack Considering the Surface Topography and the Near-Surface Velocity Gradient. 8th Int. Congress, Soc. Bras. Geofísica (SBGf), Expanded Abstracts.
- Hertweck, T., Jäger, C., Mann, J., and Duvencek, E. (2003). An integrated data-driven approach to seismic reflection imaging. 65th Conference & Exhibition, Europ. Assoc. Geosci. Eng., Extended Abstracts. Session P004.
- Hubral, P., editor (1999). *Macro-model independent seismic reflection imaging*, volume 42(3,4). J. Appl. Geophys.
- Jäger, R., Mann, J., Höcht, G., and Hubral, P. (2001). Common-Reflection-Surface stack: Image and attributes. *Geophysics*, 66:97–109.
- Koglin, I. and Ewig, E. (2003). Residual static correction by means of CRS attributes. 73rd Annual Internat. Mtg., Soc. Expl. Geophys., Expanded Abstracts. Session SP 1.4.
- Mann, J. (2002). *Extensions and Applications of the Common-Reflection-Surface Stack Method*. Logos Verlag, Berlin.
- Mann, J., Duvencek, E., Hertweck, T., and Jäger, C. (2003). A seismic reflection imaging workflow based on the Common-Reflection-Surface stack. *J. Seis. Expl.*, 12:283–295.
- Müller, T. (1999). *The Common Reflection Surface Stack Method – Seismic imaging without explicit knowledge of the velocity model*. Der Andere Verlag, Bad Iburg.
- Vieth, K.-U. (2001). *Kinematic wavefield attributes in seismic imaging*. PhD thesis, University of Karlsruhe, Germany. <http://www.ubka.uni-karlsruhe.de/vvv/2001/physik/2/2.pdf>.

Acknowledgments

This work was kindly supported by HotRock EWK Offenburg/Pfalz GmbH, Karlsruhe, Germany, the Federal Ministry for the Environment, Nature Conservation and Nuclear Safety (BMU), Germany, and the sponsors of the Wave Inversion Technology (WIT) Consortium, Karlsruhe, Germany. The authors also would like to thank Deutsche Montan Technologie (DMT) GmbH, Essen, Germany, for the fruitful collaboration during this project.